TRANSACTIONS ON EMERGING TELECOMMUNICATIONS TECHNOLOGIES
Trans. Emerging Tel. Tech. 2015; **26**:389–402
Published online 14 February 2013 in Wiley Online Library (wileyonlinelibrary.com). DOI: 10.1002/ett.2620

RESEARCH ARTICLE

SNR-dependent radius control sphere detection for MIMO systems and relay networks†

Shuangshuang Han[1], Chintha Tellambura[1]* and Tao Cui[2]

[1] Department of Electrical and Computer Engineering, University of Alberta, Edmonton, AB, Canada T6G 2V4
[2] Department of Electrical Engineering, California Institute of Technology, Pasadena, CA 91125, USA

ABSTRACT

A new sphere decoder algorithm for uncoded spatial multiplexing multiple-input multiple-output (MIMO) systems is proposed. It overcomes the drawbacks of traditional sphere decoders: variable complexity and high complexity in low signal-to-noise ratios (SNRs). Its main novelty lies in scaling the search radius by a heuristic SNR-dependent factor. This new SNR-dependent radius control sphere decoder offers near maximum likelihood performance over the entire range of SNRs, while keeping its complexity roughly constant. This algorithm also incorporates channel ordering to save complexity. To quantify the variability of complexity, the normalised variance of the complexity is evaluated. This algorithm is also extended for joint iterative detection and decoding in coded MIMO systems and for MIMO-relay networks. Simulation results and theoretical analysis demonstrate the benefits of the proposed algorithm. Copyright © 2013 John Wiley & Sons, Ltd.

***Correspondence**
C. Tellambura, Department of Electrical and Computer Engineering, University Alberta, Edmonton, AB, Canada T6G 2V4.
E-mail: chintha@ece.ualberta.ca

†This paper was presented in part at the IEEE International Conference on Communications (ICC), June 2011, Kyoto, Japan.

Received 31 July 2012; Revised 31 December 2012; Accepted 6 January 2013

1. INTRODUCTION

Spatial multiplexing multiple-input multiple-output (MIMO) systems over a rich-scattering wireless channel are capable of providing enormous capacity improvements without increasing the bandwidth or transmit power. These systems, however, require a maximum likelihood (ML) detector. Because the naive ML detector uses an exhaustive search, its complexity grows exponentially with the number of transmit antennas and with the order of the signal constellation. The alternatives are the Fincke–Pohst (FP) and the more efficient Schnorr–Euchner (SE) sphere decoders [1], which achieve ML-performance with reduced complexity, especially for the high signal-to-noise ratio (SNR) region.

Nevertheless, the sphere decoders suffer from (i) high complexity in the low SNR region and (ii) a high variability in complexity as a function of the SNR. To address these challenges, many variants have been developed [1–14]. For example, [3] uses conditional probabilities to select more reliable candidates, but the complexity is still high for near-ML performance and for high-order constellations. Statistical pruning approaches [4, 6, 7] sacrifice performance for complexity reduction. K-best, [8] also known as the M-algorithm [15] or as beam search in the Artificial Intelligence literature [16], and the fixed complexity (Fixed) [9, 17] have also been proposed. K-best traverses the search space in a breadth-first manner and retains only several best nodes in each level. Despite its fixed complexity, K-best requires higher complexity than that of the naive sphere decoder for exact ML performance [8]. Although Fixed ensures a fixed complexity, regardless of the noise level and channel conditions, it has higher complexity than that of SE in the high SNR regime [9]. Many adaptive methods have also been developed including search radius adjustments [18–21], channel-adaptive MIMO detection [22] and an early-pruned K-best algorithm [23].

Sphere decoder is also required to provide soft information for coded MIMO systems. One jointly iterative detection and decoding method has been proposed [24], which uses a list version of sphere decoder (LSD) for coded MIMO systems. In this scheme, the error correction code (ECC) can be any code that can be decoded by using soft inputs and outputs, such as convolutional codes or turbo

codes. Many algorithms are capable of supporting soft outputs in LSD. For example, K-best has been extended for use in an iterative MIMO receiver [8], and a list Fixed sphere decoder has been proposed [25] as a list extension of the Fixed algorithm [9] for coded MIMO systems.

Sphere decoder is also required for MIMO-relay networks. The benefits of relays [26] are (i) increased diversity, (ii) increased code rates, (iii) reduction of transmit power and (iv) extension of coverage area. The relay detection problem has thus been considered [27] for detect (or decode)-and-forward (DF) relaying and amplify-and-forward (AF) relaying. Low-complexity detection by applying zero-forcing at the relay terminals [28] fails to achieve ML performance. To achieve near-ML performance, detection at DF relays is computationally intensive; thus, cooperative partial detection (CPD) has been proposed [29]. The relay in this case detects a subset of transmit symbols, and only these are relayed to the destination. Although the complexity is low, this method performs poorly when the number of detected symbols is small [29].

In this paper, we propose a new SNR-dependent radius control sphere decoder (SRC-SD), which is also applied for soft MIMO detection and MIMO-relay detection.

Contributions:

(1) A new SRC-SD with a low and roughly fixed level of complexity over the whole SNR region and near-ML performance is proposed. It scales the search radius by a heuristic SNR-dependent factor. This factor approaches one in the high SNR region guaranteeing that SRC-SD's performance converges to that of the conventional sphere decoder; however, in the low SNR region, this factor is less than unity, resulting more pruning of nodes and thereby significantly reducing the complexity.
(2) A soft version for coded MIMO systems is developed with a list SRC-SD (LSRC-SD), which generates a list of candidates and further reduces the complexity of iterative detection at a negligible performance loss.
(3) To leverage the benefits of our new SRC-SD, its use in MIMO AF and DF relays is developed by deriving the ML detection rules.
(4) By considering the average number of visited nodes as a measure of complexity, an upper bound to the complexity of the proposed SRC-SD is derived. This theoretical result along with the simulation results confirms the complexity savings of SRC-SD.
(5) A measure η of the variability of complexity for the range of SNR is defined. If η is zero, then the complexity is fixed, an ideal state. The η values of the proposed SRC-SD and the conventional sphere decoders are then examined, and the very low variability of the proposed algorithm is established.

The rest of this paper is organised as follows. Section 2 describes the system models of a MIMO system, a coded MIMO system and a multibranch dual-hop MIMO-relay network. Section 3 briefly outlines the conventional sphere decoder and derives the new SRC-SD. Section 4 derives coded MIMO detection and the ML rules for MIMO-relay networks. Section 5 provides a brief complexity analysis. Simulation results for both performance and complexity are presented in Section 6, followed by the conclusions in Section 7.

2. SYSTEM MODELS

2.1. Standard multiple-input multiple-output maximum likelihood detection

A spatial multiplexing MIMO system with N transmit antennas and N receive antennas is considered. A rich-scattering memoryless (flat fading) channel is assumed. The transmitted symbol vector consists of N symbols from a constellation $\mathcal{Q}$ [a complex constellation such as 16-quadrature amplitude modulation (QAM)]. The MIMO channel is an $N \times N$ Rayleigh fading channel matrix with independent identically distributed elements $h_{ij} \sim \mathcal{CN}(0,1)$, where $\mathcal{CN}(0,1)$ is a complex Gaussian variable with zero mean and unit variance. As usual, the channel matrix is assumed to be perfectly known by the receiver. By factorising the channel matrix and preprocessing the received signal appropriately, the ML detection rule for the equivalent real system may be given as [1]

$$\hat{\mathbf{s}} = \arg\min_{\mathbf{s}\in\Omega^m} \|\mathbf{z} - \mathbf{R}\mathbf{s}\|^2 \tag{1}$$

where $m = 2N$, and $\mathbf{R}$ is an $m \times m$ upper-triangular matrix, which is obtained by QR factorization of the real channel matrix. $\mathbf{z}$ is obtained by received signal $\mathbf{y}$ and $\mathbf{Q}$, where $\mathbf{z} = \mathbf{Q}^H\mathbf{y}$. $\|x\|$ represents the Frobenius norm of x. Ω^m is the m dimensional vector of symbols from the real constellation Ω. For example, 16-QAM can be transformed to two real 4-pulse amplitude modulation (PAM) constellations with $\Omega = \{-3, -1, 1, 3\}$. The details of this well-known model are omitted for brevity; for further details, the interested reader is referred to [1]. Note that the exhaustive search of (1) has a complexity $O(|\Omega|^m)$.

2.2. Coded multiple-input multiple-output model

We consider a coded spatial multiplexing MIMO system (Figure 1). Information vector $\mathbf{b}$ as a frame of M_b bits are encoded by the ECC module, whose output $\mathbf{c}$ goes through an interleaver Π. ECC can be a convolutional code or a turbo code in particular with code rate R; thus, the length of the coded sequence $\mathbf{c}$ is $M_c = M_b/R$. The interleaver here ensures statistical independence. The interleaved bits $\underline{\mathbf{x}}$ are modulated to channel symbols $\underline{\mathbf{s}}$ and transmitted. M_x and M_s are the frame length of $\underline{\mathbf{x}}$ and $\underline{\mathbf{s}}$, respectively, where $M_x = M_s \log_2(|\mathcal{Q}|)$. Therefore, a frame of M_s symbols

Trans. Emerging Tel. Tech. **26**:389–402 (2015)
DOI: 10.1002/ett

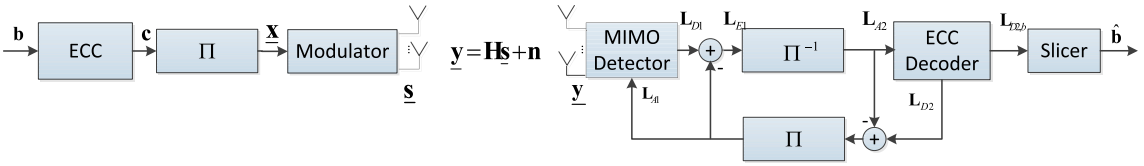

Figure 1. The system model of iterative detection and decoding. ECC, error correction code; MIMO, multiple-input multiple-output.

requires the transmission of $M_{ch} = M_s/N$ blocks of data, corresponding to M_{ch} different channel realisations.

At the receiver, several iterations of soft information exchange [24] occur between the ECC decoder and MIMO detector. The MIMO detector in this case generates soft a posteriori information $\mathbf{L}_{D1}$ by processing the received signal $\underline{\mathbf{y}}$ and the a priori information $\mathbf{L}_{A1}$ from the ECC decoder. This reliability information is expressed by a posteriori probability in the form of log-likelihood ratios (LLR). For example, the LLR of bit $\underline{x}_i (i = 1, 2, \ldots, M_x)$ is defined as

$$L(\underline{x}_i) = \ln \frac{\Pr[\underline{x}_i = +1]}{\Pr[\underline{x}_i = -1]} \tag{2}$$

Note that the amplitude levels -1 and $+1$ represent binary 0 and 1, respectively.

For the first iteration, the $\mathbf{L}_{A1}$ is initialized to 0, and the *extrinsic* information $\mathbf{L}_{E1} = \mathbf{L}_{D1} - \mathbf{L}_{A1}$ generated by the MIMO detector is deinterleaved by Π^{-1} to serve as the a priori information for the ECC decoder. The ECC decoder then generates the extrinsic information for the next iteration. This process continues until a stopping criterion is met, such as a predefined iteration number or a performance bound. In the final iteration, the ECC decoder obtains the a posteriori information $\mathbf{L}_{D2,b}$ on the uncoded bits $\mathbf{b}$ [30], which is sent to the slicer that outputs the final bit estimates $\hat{\mathbf{b}}$.

2.3. Relay network model

A basic system model for a multibranch dual-hop relay network is considered, which contains the source ($\mathbb{S}$), N_{re} relays ($\mathbb{R}$) and the destination ($\mathbb{D}$), where N_{re} is the number of relays in the network. The number of antennas at the source, the relays and the destination terminal are denoted as N_s, N_r and N_d, respectively. All nodes are half-duplex and use orthogonal channels, and a direct link exists from the source to the destination. Relay protocols operate in two time slots. In the first time slot, the source broadcasts its message to all the relays and the destination. In the second time slot, the relays transmit the received and/or processed signals to the destination.

The channels between the source and the ith relay, the ith relay and the destination, the source and the destination are denoted by $\mathbf{H}_{sr}^{(i)} \in \mathcal{C}^{N_r \times N_s}$, $\mathbf{H}_{rd}^{(i)} \in \mathcal{C}^{N_d \times N_r} (i \in \{1, 2, \ldots N_{re}\})$ and $\mathbf{H}_{sd} \in \mathcal{C}^{N_d \times N_s}$, where $\mathcal{C}$ is the set of complex numbers. For the first time slot, the received signal vector at the ith relay ($i = 1, 2, \ldots, N_{re}$) and the destination are given by

$$\mathbf{y}_{sr}^{(i)} = \mathbf{H}_{sr}^{(i)} \mathbf{s}_s + \mathbf{n}_{sr}^{(i)} \tag{3}$$

$$\mathbf{y}_{sd} = \mathbf{H}_{sd} \mathbf{s}_s + \mathbf{n}_{sd} \tag{4}$$

where $\mathbf{s}_s$ and $\mathbf{n}_{sr}^{(i)}, \mathbf{n}_{sd} \sim \mathcal{CN}(0, 1)$ are the transmitted signal at the source, the additive white Gaussian noise (AWGN) at the ith relay ($i = 1, 2, \ldots, N_{re}$) and the destination, respectively.

As before, the channel matrix entries are assumed to be independent elements. To be exact, the entries are $\mathcal{CN}\left(0, \frac{\mathrm{SNR}_{sr}^{(i)}}{N_s}\right)$, $\mathcal{CN}\left(0, \frac{\mathrm{SNR}_{rd}^{(i)}}{N_r}\right)$, $\mathcal{CN}\left(0, \frac{\mathrm{SNR}_{sd}}{N_s}\right)$ for $\mathbf{H}_{sr}^{(i)}$, $\mathbf{H}_{rd}^{(i)}$ and $\mathbf{H}_{sd}$, respectively. The SNRs are defined to be consistent with [29] to be $\frac{\mu P}{\left(d_{sr}^{(i)}\right)^{\alpha}}$, $\frac{(1-\mu)P}{\left(d_{rd}^{(i)}\right)^{\alpha}}$, $\frac{\mu P}{(d_{sd})^{\alpha}}$, respectively. where $\mu \in (0, 1]$ denotes the proportion factor of transmit power between the source and the relays; the equivalent power and distance to the source at all the relays are assumed; $d_{sr}^{(i)}$, $d_{rd}^{(i)}$ and d_{sd} denote the distance between the source and the ith relay, the ith relay and the destination, the source and the destination, respectively; P is the total power for the source and the relays, and $\alpha \in [2, 6]$ is the path loss exponent.

2.3.1. Detect-and-forward relaying.

We focus on detection strategies for the relay networks and assume that the channel state information is available at all the nodes and could be established from the transmitted pilot symbols. Similar to the system model demonstrated in [29], we have not considered the errors resulted by the detection at the relays to compare our method with the method [29].

The relays process and forward the received signal from the source (3) to the destination. Thus, at the end of the second time slot, the received signal vector at the destination from the ith relay ($i = 1, 2, \ldots, N_{re}$) is given as

$$\mathbf{y}_{rd}^{(i)} = \mathbf{H}_{rd}^{(i)} \mathbf{s}_r^{(i)} + \mathbf{n}_{rd}^{(i)} \tag{5}$$

where $\mathbf{s}_r^{(i)}$ is the signal detected at the ith relay by using sphere decoder, and $\mathbf{n}_{rd}^{(i)} \sim \mathcal{CN}(0, 1)$ is an AWGN sample.

2.3.2. Amplify-and-forward relaying.

The relays just amplify the received signals (3) from the source during the first time slot and retransmit to

the destination during the second time slot. The ith relay ($i = 1, 2, \ldots, N_{re}$) amplifies $\mathbf{y}_{sr}^{(i)}$ by a fixed gain parameter α_i [31], which is chosen to satisfy the power constraint. Therefore, the received signal at the destination from the ith relay, $i = 1, 2, \ldots, N_{re}$, is

$$\begin{aligned}\mathbf{y}_{rd}^{(i)} &= \mathbf{H}_{rd}^{(i)}\left(\alpha_i \mathbf{y}_{sr}^{(i)}\right) + \mathbf{n}_{rd}^{(i)} \\ &= \alpha_i \mathbf{H}_{rd}^{(i)}\mathbf{H}_{sr}^{(i)}\mathbf{s}_s + \mathbf{n}^{'}\end{aligned} \tag{6}$$

where the noise term $\mathbf{n}^{'} = \alpha_i \mathbf{H}_{rd}^{(i)}\mathbf{n}_{sr}^{(i)} + \mathbf{n}_{rd}^{(i)}$.

For both DF and AF modes, the destination terminal combines the received signals from the source $\mathbf{y}_{sd}$ (4) and the relays $\mathbf{y}_{rd}^{(i)}$, $i = 1, 2, \ldots, N_{re}$, and performs ML detection.

3. SIGNAL-TO-NOISE RATIO-DEPENDENT DETECTION

This section briefly introduces the conventional sphere decoder and proposes the new SRC-SD. Complexity analysis and quantifying the variability of complexity are discussed.

3.1. Conventional sphere decoder

The real-system formulation is used to briefly explain the basic FP and SE sphere decoders. (see [1] for more details.) Both of these algorithms restrict the search space to a hypersphere within a radius d centred around the received signal. To generate the points inside the hypersphere, all points $\mathbf{s}$ such that $\|\mathbf{z} - \mathbf{Rs}\|^2 \leqslant d^2$ can be expanded as $\sum_{i=1}^{m}\left(z_i - \sum_{j=i}^{m} r_{i,j}s_j\right)^2 \leqslant d^2$. This inequality can be replaced by a set of looser bounds. In the Pohst enumeration [32], for example, given the symbols $s_{i+1}, \ldots, s_m$, the element s_i can be chosen from the range of $LB_i \leqslant s_i \leqslant UB_i$ where

$$LB_i = \left\lceil \frac{1}{r_{i,i}}\left(z_i - \sum_{j=i+1}^{m} r_{i,j}s_j - d_i\right)\right\rceil \tag{7}$$

$$UB_i = \left\lfloor \frac{1}{r_{i,i}}\left(z_i - \sum_{j=i+1}^{m} r_{i,j}s_j + d_i\right)\right\rfloor \tag{8}$$

with $d_i^2 = d^2 - \sum_{k=i+1}^{m}\left(z_k - \sum_{j=k}^{m} r_{k,j}s_j\right)^2$, where $\lceil x \rceil$ is the smallest integer greater than or equal to x, and $\lfloor x \rfloor$ is the largest integer less than or equal to x. In the SE enumeration [33], the admissible points are searched in a zigzag order from the midpoint $s_{i,\text{mid}} = \left\lceil \frac{1}{r_{i,i}}(z_i - d_i)\right\rfloor$, where $\lceil x \rfloor$ is the nearest integer around x. The spanning order is $s_{i,\text{mid}}, s_{i,\text{mid}} + 1, s_{i,\text{mid}} - 1, s_{i,\text{mid}} + 2, \ldots$, when $z_i - d_i - r_{i,i}s_{i,\text{mid}} \geqslant 0$, and $s_{i,\text{mid}}, s_{i,\text{mid}}-1, s_{i,\text{mid}}+1, s_{i,\text{mid}}-2, \ldots$, otherwise. This enumeration method has been found to be more efficient than the Pohst enumeration.

For the original FP, the initial radius can be selected on the basis of the noise level [34]. The initial radius for SE is typically set as $d = \infty$ [1]. More results on sphere decoders may be found [2–14].

3.2. Signal-to-noise ratio-dependent scaling function

As discussed in our Introduction, although the FP and SE sphere decoders save complexity compared with the naive ML detector, their computational complexity is variable and high in the low SNR region. These two problems are mitigated by our proposed SRC-SD at a negligible performance loss.

The traditional FP and SE algorithms achieve complexity savings by pruning nodes in the search tree, but pruning is limited to nodes that can be identified early in the search to be not on the ML path. Such nodes are few and their pruning results in only modest complexity reduction, especially in the low SNR region. Therefore, to achieve substantial complexity savings, more nodes need to be pruned. To this end, our main idea is to scale the search radius of the hypersphere on the basis of the SNR, which is defined as a scaling function $\phi(\rho)$ on the basis of the SNR ρ. Several properties for the scaling factor are the following:

(1) $\phi(\rho)$ has to be a positive value for all the SNRs, $\phi(\rho) \geqslant 0$.
(2) $\phi(\rho)$ should be smaller than one to obtain complexity savings than the conventional sphere decoder, that is $\phi(\rho) \leqslant 1$.
(3) To prune more nodes in the low SNR region and to keep the optimal performance in the high SNR region, $\phi(\rho)$ should be an increasing function of ρ.
(4) When the SNR is high enough, the scaling factor approaches to one, that is, $\lim_{\rho\to\infty}\phi(\rho) = 1$ that guarantees to have the optimal performance in the high SNR region.

There are many different scaling functions, such as $1/(\exp(-\rho) + 1)$, $\rho/(\rho + C_0)$ and so forth. On the basis of numerical experiments, we propose the specific scaling function (9), which is a simple function of the SNR and efficiently achieves a nice performance and complexity trade-off.

3.3. Signal-to-noise ratio-dependent radius control sphere decoder

This decoder uses the scaling function to obtain the new radius via

$$d_{\text{SRC-SD}}^2 = \phi(\rho) \times d^2 = \frac{\rho}{\rho + C_0} \times d^2 \tag{9}$$

Trans. Emerging Tel. Tech. **26**:389–402 (2015)
DOI: 10.1002/ett

where $d_{\text{SRC-SD}}$ is the radius in the new SRC-SD, ρ is the SNR of the MIMO system, d is the radius used in the original FP or the SE, and C_0 is a predefined constant. This scaling function satisfies the conditions mentioned earlier. Because of the limit

$$\lim_{\rho\to\infty} \frac{\rho}{\rho + C_0} = 1 \tag{10}$$

the performance of the proposed algorithm reverts to that of the original sphere decoder when the SNR is sufficiently high.

When we apply this idea to the original FP, denoted by SRC-FP, its initial radius

$$\begin{aligned} d^2_{\text{SRC-FP}} &= \frac{\rho}{\rho + C_0} \times d^2 \\ &= \frac{\rho}{\rho + C_0} \times \alpha n \sigma_r^2 \\ &= \frac{\alpha n m}{4(\rho + C_0)} \end{aligned} \tag{11}$$

where $m = n = 2N$, the noise variance in real MIMO system $\sigma_r^2 = \frac{\sigma^2}{2}$ and σ^2 is the additive noise variance. The last step for (11) is based on the fact that the SNR in a complex MIMO system is given by $\rho = \frac{NE(|s|^2)}{\sigma^2}$, where the average energy of each symbol $E(|s|^2) = 1$ is assumed.

Because SE has lower complexity compared with FP, we choose the former as the building block of SRC-SD (Algorithm 1). Thus, SRC-SD is derived by augmenting the SE sphere decoder with the SNR-dependent radius (9).

To further improve the proposed SRC-SD, the ordering of the channel matrix is included in our algorithm. In lines 1–4, the algorithm iteratively reorders the m columns of the channel matrix. The main idea of reordering is that the signals suffering the smallest noise amplification should be selected in every iteration as discussed in [9, 35].

As Algorithm 1 reveals, the proposed SRC-SD is a variant of the conventional SE [1] and achieves a critical improvement in computational complexity and near-ML performance (Section 6).

3.4. Complexity analysis for SNR-dependent radius control sphere decoder

An exact complexity analysis of SRC-SD algorithm appears intractable because of the updating of radius and the zigzag search ordering, which is adapted from SE [1]. Fortunately, the complexity of SE is less than that of the FP. Thus, we evaluate the complexity of the SRC-FP sphere decoder, which will be an upper bound of the complexity of SRC-SD.

The complexity of an sphere decoder may be taken as the average number of nodes visited. This average depends on the number of antennas, the initial radius and the noise variance [34]. By considering the number of nodes visited at all the levels, the expected complexity of sphere decoder is given by

$$C\left(m, \sigma_r^2, d^2\right) = \sum_{k=1}^{m} \varphi_k \tag{13}$$

Algorithm 1: The signal-to-ratio-dependent radius control sphere decoder algorithm

Input : ρ, C_0, $\mathbf{z}$, $\mathbf{H}$
Output: $\hat{\mathbf{s}}$

1 Iteratively order the m columns of the channel matrix $\mathbf{H}$. The steps of the ordering is: **for** $i \leftarrow m$ **to** 1 **do**
2 Calculate $\mathbf{H}_i^{\dagger} = \left(\mathbf{H}_i^H \mathbf{H}_i\right)^{-1} \mathbf{H}_i^H$, where $\mathbf{H}_i$ is the channel matrix with columns selected in previous iterations zeroed;
3 The signal to be detected ($\hat{s_p}$) is obtained by

$$p = \underset{\mathbf{j}\in\{1,\ldots,m\}-\{\mathbf{p}_{i+1}\}}{\arg\min} \| \left(\mathbf{H}_i^{\dagger}\right)_j \|^2, \tag{12}$$

where $(\mathbf{H}_i^{\dagger})_j$ denotes the jth row of $\mathbf{H}_i^{\dagger}$, and $\mathbf{p}_{i+1}$ is the columns selected in previous iterations;
4 **end**
5 Order the channel $\mathbf{H}$ by the index vector $\mathbf{p}$, and get the matrix $\mathbf{R}$ by QR factorization;
6 Initial the radius $d_{SRC-SD} = \infty$ and take the root s_0 (level $k = m$) as the start node;
7 **for** *depth* $k \leftarrow m$ **to** 1 **do**
8 Expand the Current Node, generating all its successors $\mathcal{T}$ in the k-th level satisfying $\left(z_k - \sum_{j=k}^{m} r_{k,j} s_j\right)^2 \leq d^2_{SRC-SD} - \sum_{i=k+1}^{m} \left(z_i - \sum_{j=i}^{m} r_{i,j} s_j\right)^2$; Prune other successors;
9 Sort the components in $\mathcal{T}$ by the increasing order of all the branch weights c_i in this level, where $c_i = \left(z_i - r_{i,i} s_i - \sum_{j=i+1}^{m} r_{i,j} s_j\right)^2$ and $s_i \in \mathcal{T}$;
10 **for** *every element* s_i **do**
11 **if** s_i *is not a leaf node,* **then** set s_i as Current Node, $k = k - 1$ and go back to line 3;
12 **else** if s_i is a leaf node ($k = 1$), and if its cost is lower than d^2_{SRC-SD}, keep it as the best solution and update d^2_{SRC-SD} by (9).
13 **end**
14 **end**

where φ_k is the number of nodes visited at kth level within the hypersphere of radius d.

Furthermore, here, we show only the theoretical complexity for 16-QAM, which is equivalent to two real 4-PAM constellations. Other constellations may be analysed similarly but are omitted for the sake of brevity. For consistency with the results of [34], the average energy of the transmitted signals is not set to one. Therefore, by using [34, Theorem 2] and the SNR-dependent radius $d^2_{\text{SRC-SD}}$ (11), the expected complexity of SRC-FP is given as Equation (14), where $g_{kl}(q)$ is the coefficient of x^q in the polynomial $(1 + x + x^4 + x^9)^l(1 + 2x + x^4)^{k-l}$, and $\sigma_r^2 = \frac{m}{\rho} \times \frac{L^2-1}{12}$ (for 4-PAM, $L = 4$).

$$C_{\text{SRC-FP}}(m, \rho, C_0) = \sum_{k=1}^{m} \sum_{q} \frac{1}{2^k} \sum_{l=0}^{k} \binom{k}{l} \times g_{kl}(q) \gamma \left(\frac{\alpha n \rho}{2(\rho + C_0)\left(1 + \frac{12\rho q}{m(L^2-1)}\right)}, \frac{n-m+k}{2} \right) \tag{14}$$

3.5. Variability of complexity

Complexity C is a random variable. We are interested in its variability for different SNRs. The variability index η is thus proposed as the ratio between the variance of C and square mean of C:

$$\eta = \frac{E(C - \bar{C})^2}{\bar{C}^2} \tag{15}$$

where C denotes the complexity measured by the average number of nodes visited by sphere decoder; $\bar{C}$ and $E(C)$ denote the mean and the expectation of C for all the SNRs, respectively.

Therefore, the smaller the index, the less is the variability of the complexity. For example, from the aforementioned theoretical analysis, the FP and SRC-FP ($C_0 = 5$ as an example) sphere decoders achieve $\eta = 1.78$ and $\eta = 0.69$, respectively. The reduced value η suggests that SRC-FP achieves a more constant level of complexity than the original FP.

Remarks

(1) The new SRC-SD has lowered the computational complexity compared with the basic sphere decoder, especially in the low SNR region, while maintaining near-ML performance in the high SNR region. The channel-ordering method in lines 1–4 of Algorithm 1 is included to further reduce the complexity.
(2) The new SRC-SD effectively reduces the variability index η, which is particularly helpful for hardware implementation.
(3) This idea of an SNR-dependent radius can also be applied to other types of tree search algorithms for MIMO detection, such as many sphere decoder variants [3, 7] or different stopping criteria [36].
(4) We have not discussed in detail the effects of the constant C_0 in Equation (9), which should be adjusted for different systems. For adjusting C_0, we can use the conventional SE as a guide. When the SNR is large enough, say 20 dB, it has a very low complexity and further complexity reductions appear not possible. Thus, a smaller C_0 may be chosen so that SRC-SD performs close to SE in the high SNR regime.

4. DETECTION STRATEGIES

This section introduces coded MIMO detection and MIMO-relay detect strategies. For both AF and DF relays, the ML rule for combining the received signals from the relays and the source is derived.

4.1. Soft multiple-input multiple-output detection

For simplicity, we consider a block of bits $\underline{\mathbf{x}}$ with $N_B = N \log_2(|\mathcal{Q}|)$, where N_B is the number of bits in one block. The optimal detector obtains the exact a posteriori probability for each bit, the a posteriori LLRs of the bits $\underline{x}_k$ ($k = 1, 2, \ldots, N_B$) conditioned on the received signal vector $\underline{\mathbf{y}}$ [24] is

$$\begin{aligned} L_{D1}(\underline{x}_k|\underline{\mathbf{y}}) &= \ln \frac{\Pr[\underline{x}_k = +1|\underline{\mathbf{y}}]}{\Pr[\underline{x}_k = -1|\underline{\mathbf{y}}]} \\ &= L_{A1}(\underline{x}_k) + L_{E1}(\underline{x}_k|\underline{\mathbf{y}}) \end{aligned} \tag{16}$$

Here, the Bayes' theorem and the independence of the bits $\underline{x}_k$ due to the interleaver are used to obtain the a priori LLRs $L_{A1}(\underline{x}_k)$ and the *extrinsic* LLRs $L_{E1}(\underline{x}_k|\underline{\mathbf{y}})$. From [24], the *extrinsic* information can be denoted by Equation (17) on next page. It is obtained by applying the definition of the extrinsic information [24] and the Max-log approximation [37]. Here, $\mathbb{X}_{k,+1}$ and $\mathbb{X}_{k,-1}$ denote the sets of the bit vectors $\underline{\mathbf{x}} = \left(\underline{x}_1, \underline{x}_2, \ldots, \underline{x}_{N_B}\right)^T$ having $\underline{x}_k = +1$ and $\underline{x}_k = -1$, respectively. $\mathbf{x}_{[k]}$ represents the subvector of $\underline{\mathbf{x}}$ by omitting the kth bits $\underline{x}_k$; $\mathbf{L}_{A1[k]}$ denotes the subvector of $\mathbf{L}_{A1} = \left(L_{A1}(\underline{x}_1), L_{A1}(\underline{x}_2), \ldots, L_{A1}(\underline{x}_{N_B})\right)^T$ by omitting the $L_{A1}(\underline{x}_k)$.

Despite these simplifications, the computing of $L_{E1}(\underline{x}_k|\underline{\mathbf{y}})$ (17) has an exponential complexity $O(|\mathcal{Q}|^N)$ and is prohibitively complex for systems with a large number of antennas and with high-order modulations. Therefore, we develop a list version of SRC-SD.

List SRC-SD generates a list $\mathcal{L}$ of $N_{\mathcal{L}}$ candidates by searching the tree by using a rule. This list includes the ML estimate, but the size of the list satisfies $1 \leqslant N_{\mathcal{L}} < 2^{N_c \cdot N}$, where $N_c = \log_2(|\mathcal{Q}|)$ is the number of bits per modulated symbol. Therefore, to compute the $L_{E1}(\underline{x}_k|\underline{\mathbf{y}})$, the searching space in Equation (17) is limited in the list $\mathcal{L}$, and the extrinsic information can be rewritten as Equation (18), where $\mathcal{L} \cap \mathbb{X}_{k,+1}$ and $\mathcal{L} \cap \mathbb{X}_{k,-1}$ represent the subset of vectors $\mathcal{L}$ having $\underline{x}_k = +1$ and $\underline{x}_k = -1$, respectively.

List SRC-SD is a soft extension of SRC-SD, which is used to obtain the set of candidates around the ML estimate that can be exploited to calculate the soft extrinsic information of Equation (17) for the iterative detection and decoding. Our LSRC-SD significantly reduces the complexity of generating the candidate list $\mathcal{L}$ by adopting several properties of the classical LSD [24]. First, the radius is updated whenever a better candidate than the worst candidate in the current list is found. Second, the candidate list is not generated for every iteration. Once computed, it is stored in the memory and used by every iteration. Therefore, for every iteration, the only information needing to be updated is the a priori information from the channel decoder.

$$L_{E1}(\underline{x}_k|\underline{\mathbf{y}}) \approx \frac{1}{2}\max_{\underline{\mathbf{x}}\in\mathbb{X}_{k,+1}}\left\{\underline{\mathbf{x}}_{[k]}^T\mathbf{L}_{A1[k]} - \frac{1}{\sigma^2/2}\|\underline{\mathbf{y}} - \mathbf{H}\underline{\mathbf{s}}\|^2\right\} - \frac{1}{2}\max_{\mathbf{x}\in\mathbb{X}_{k,-1}}\left\{\underline{\mathbf{x}}_{[k]}^T\mathbf{L}_{A1[k]} - \frac{1}{\sigma^2/2}\|\underline{\mathbf{y}} - \mathbf{H}\underline{\mathbf{s}}\|^2\right\} \quad (17)$$

$$L_{E1}(\underline{x}_k|\underline{\mathbf{y}}) \approx \frac{1}{2}\max_{\underline{\mathbf{x}}\in\mathcal{L}\cap\mathbb{X}_{k,+1}}\left\{\underline{\mathbf{x}}_{[k]}^T\mathbf{L}_{A1[k]} - \frac{1}{\sigma^2/2}\|\underline{\mathbf{y}} - \mathbf{H}\underline{\mathbf{s}}\|^2\right\} - \frac{1}{2}\max_{\underline{\mathbf{x}}\in\mathcal{L}\cap\mathbb{X}_{k,-1}}\left\{\underline{\mathbf{x}}_{[k]}^T\mathbf{L}_{A1[k]} - \frac{1}{\sigma^2/2}\|\underline{\mathbf{y}} - \mathbf{H}\underline{\mathbf{s}}\|^2\right\} \quad (18)$$

Similar to the a posteriori information of the MIMO detector, that of the channel decoder can also be decomposed into the a priori information and extrinsic information for the iterative detection and decoding. Therefore, the details of the channel decoder are not shown in this paper.

4.2. Multiple-input multiple-output-relay detection

For single-relay networks with DF relaying, ML detection at the relay and destination is proposed in [29]. This section considers DF and AF relays.

4.2.1. Detect-and-forward relaying.

The detection problem at each relay is equivalent to the standard MIMO detection problem (1). For the first step at the ith relay ($i = 1, 2, \ldots, N_{re}$), the ML detection rule is thus given by

$$\mathbf{s}_r^{(i)} = \arg\min_{\mathbf{s}_s\in\mathcal{Q}^{N_s}} ||\mathbf{y}_{sr}^{(i)} - \mathbf{H}_{sr}^{(i)}\mathbf{s}_s||^2 \quad (19)$$

where $\mathcal{Q}^{N_s}$ is the set of constellation symbols in the N_s dimensional constellation $\mathcal{Q}$. The computational complexity is significantly reduced by using sphere decoder. On the basis of Equation (19) and the QR factorization of $\mathbf{H}_{sr}^{(i)}$ $\left(\mathbf{H}_{sr}^{(i)} = \mathbf{Q}_{sr}^{(i)}\mathbf{R}_{sr}^{(i)}\right)$ and $\mathbf{z}_{sr}^{(i)} = \mathbf{Q}_{sr}^{(i)H}\mathbf{y}_{sr}^{(i)}$, (19) is equivalent to

$$\mathbf{s}_r^{(i)} = \arg\min_{\mathbf{s}_s\in\Phi} ||\mathbf{z}_{sr} - \mathbf{R}_{sr}^{(i)}\mathbf{s}_s||^2 \quad (20)$$

Φ should be the set of all points in the hypersphere with radius d that satisfies $||\mathbf{z}_{sr}^{(i)} - \mathbf{R}_{sr}^{(i)}\mathbf{s}_{sr}^{(i)}||^2 \leqslant d^2$.

In the second step, the relays transmit to the destination. Hence, the destination receives a total of $N_{re} + 1$ signals, including the direct source signal. All these signals are combined via the ML rule as

$$\hat{\mathbf{s}}_d = \arg\min_{\mathbf{s}_s\in\mathcal{Q}^{N_s}}\left(\sum_{i=1}^{N_{re}} ||\mathbf{y}_{rd}^{(i)} - \mathbf{H}_{rd}^{(i)}\mathbf{s}_s||^2 + ||\mathbf{y}_d - \mathbf{H}_{sd}\mathbf{s}_s||^2\right) \quad (21)$$

By expanding each of the norms and regrouping some terms, the equivalent channel matrix $\mathbf{H}'$ and the equivalent received signal $\mathbf{y}'$ are derived as (see Appendix A)

$$\mathbf{H}' = \left(\sum_{i=1}^{N_{re}} \mathbf{H}_{rd}^{(i)H}\mathbf{H}_{rd}^{(i)} + \mathbf{H}_{sd}^H\mathbf{H}_{sd}\right)^{1/2} \quad (22a)$$

$$\mathbf{y}' = (\mathbf{H}')^{-1}\left(\sum_{i=1}^{N_{re}} \mathbf{H}_{rd}^{(i)H}\mathbf{y}_{rd}^{(i)} + \mathbf{H}_{sd}^H\mathbf{y}_{sd}\right) \quad (22b)$$

The ML rule is then derived by Equation (19). The difference is that sphere decoder at the destination is performed by the newly combined matrix of the channel matrix and received signal vector from Equations (22a) and (22b).

4.2.2. Amplify-and-forward relaying.

The relays simply retransmit a scaled version of the received signal. Similar to the DF relaying case (Appendix A), the equivalent channel matrix and received signal at the destination in AF relaying are given by

$$\mathbf{H}' = \left(\sum_{i=1}^{N_{re}} \left(\alpha_i\mathbf{H}_{rd}^{(i)}\mathbf{H}_{sr}^{(i)}\right)^H\left(\alpha_i\mathbf{H}_{rd}^{(i)}\mathbf{H}_{sr}^{(i)}\right) + \mathbf{H}_{sd}^H\mathbf{H}_{sd}\right)^{\frac{1}{2}} \quad (23a)$$

$$\mathbf{y}' = (\mathbf{H}')^{-1}\left(\sum_{i=1}^{N_{re}} \left(\alpha_i\mathbf{H}_{rd}^{(i)}\mathbf{H}_{sr}^{(i)}\right)^H\mathbf{y}_{rd}^{(i)} + \mathbf{H}_{sd}^H\mathbf{y}_{sd}\right) \quad (23b)$$

To sum up, sphere decoder is appropriate for the receiver in both DF relaying and AF relaying networks to reduce the complexity with near-ML performance.

Therefore, SRC-SD works for both DF and AF systems. Thus, the computational complexity at both the relays and the destination can be reduced. Previously, the Fixed algorithm [9] has been applied to obtain the fixed complexity in the MIMO-relay networks. In our results section, both the Fixed and SRC-SD algorithms will be compared.

5. COMPLEXITY ANALYSIS

The average complexity for coded MIMO and MIMO-relay detection is analysed here.

5.1. Coded multiple-input multiple-output system

For the proposed LSRC-SD, we evaluate the computational complexity of generating the candidate list. This enables a comparison of our proposed LSRC-SD and the original LSD [24].

5.2. Multiple-input multiple-output-relay networks

We now use sphere decoder for both DF and AF relays networks. For AF relays, because signal detection is not required, the complexity is the same as that of a point-to-point MIMO link (13). The DF relays require signal detection at both the relays and the destination, so the average number of nodes visited by sphere decoder algorithms is given by

$$C_{\text{all}} = \sum_{i=1}^{N_{re}} C_i + C_d \tag{24}$$

where C_i is the complexity evaluated at the ith relay ($i = 1, 2, \ldots, N_{re}$), C_d is the complexity of detection at the destination, and C_i and C_d are given by Equation (13).

6. RESULTS AND DISCUSSIONS

6.1. Multiple-input multiple-output detection

This section evaluates the performance and complexity of the proposed SRC-SD (Algorithm 1). An uncoded 4×4 MIMO 16-QAM system is considered over a flat Rayleigh fading channel. To verify the advantages of SRC-SD, both the performance measured by the error rate [e.g. symbol error rate (SER)] and the complexity measured by the average number of nodes visited of the new SRC-SD are compared with those of the FP, SRC-FP, K-best [8] and Fixed [9] sphere decoders. The first two require the choice of an initial radius, and we use the method of [34] to set the probability of the lattice point inside the sphere at $1 - \varepsilon = 0.9999$. The K-best algorithm with $K = 4$ [8], and Fixed with $p = 1$ (p is the number of levels with full enumeration and $p \geq \sqrt{N} - 1$) [9] for achieving the same diversity as ML detection are compared here. We choose C_0 to be 10 for the proposed SRC-SD where necessary.

Complexity comparison: Because computational complexity is the most important issue for implementation, it is compared for the FP, SRC-FP, SE and SRC-SD algorithms for different numbers of antennas (Figure 2). From this figure, two main observations can be found as follows:

(1) The simulation and theoretical results of both FP and SRC-FP agree, confirming the theoretical analysis of Equation (14). In this figure, an example at an SNR of 0 dB is shown. Clearly, SRC-FP achieves lower complexity than the original FP. Furthermore, the complexity gap between these two algorithms increases with the number of antennas. For example, when the number of antennas increases from three to five, the complexity gap increases by a factor of 200. This result shows that augmenting the traditional FP sphere decoder with our SNR-dependent idea achieves substantial complexity gains.

(2) The complexity of the proposed SRC-SD is also shown here, which achieves the lowest complexity for all the antenna numbers. For example, for an 8×8 MIMO system at an SNR of 0 dB, the SRC-SD, SE and FP sphere decoders search on average about 2.4×10^2, 10^5 and 10^9, respectively. Thus, over six orders of magnitude of complexity savings are achieved, confirming the high efficiency in the low SNR region of SRC-SD and affirming its suitability for large MIMO systems. Furthermore, the complexity savings depend on the operating SNR and diminish for high SNRs.

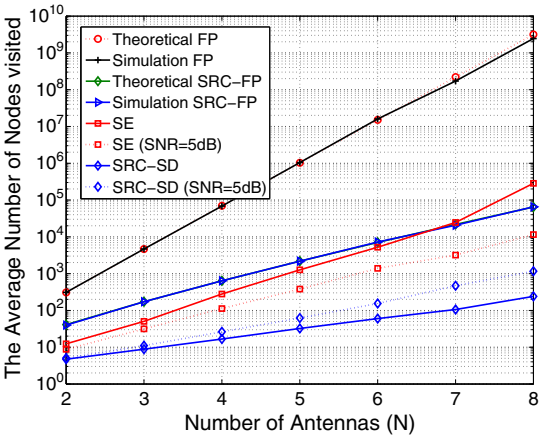

Figure 2. Comparison of different sphere decoders (16-QAM) as a function of the number of antennas, where SNR = 0 dB except stated. QAM, quadrature amplitude modulation; FP, Fincke–Pohst; SNR, signal-to-noise ratio; SE, Schnorr–Euchner; SRC-SD, SNR-dependent radius control sphere decoder.

Trans. Emerging Tel. Tech. **26**:389–402 (2015)
DOI: 10.1002/ett

How complexity varies as a function of the SNR is an important consideration (Figure 3). In this figure, the SRC-SD with/without channel ordering are compared with the FP, SE, K-best and Fixed sphere decoders. The SRC-SD with channel ordering obtains complexity saving compared with that without channel ordering. In the following, SRC-SD denotes the algorithm with channel ordering for simplicity. From this figure, the advantages of the proposed SRC-SD can be found in the following:

(1) SRC-SD significantly reduces the complexity compared with the conventional SE and FP sphere decoders. For example, for an SNR of 20 dB, SRC-SD obtains about one order of magnitude complexity savings compared with FP; and this amount increases to four orders of magnitude at 0 dB. In contrast to SE, which visits 3×10^2 nodes, SRC-SD visits only 16 nodes at 0 dB. This advantage may, however, vanish if the SNR increases, as per Equation (10).
(2) More importantly, SRC-SD also has even lower complexity than the K-best [8] and Fixed [9] sphere decoders.
(3) Notice how flat the complexity curve of SRC-SD is; the variability index η of 0.14 for SRC-SD verifies the roughly fixed complexity according to Equation (15). SRC-SD thus achieves a roughly fixed and reduced complexity.

Because of the trade-off between complexity and performance, the performance of SRC-SD is examined next.

Symbol error rate performance: Pruning the nodes by using SNR-dependent scaling of the hypersphere radius in the proposed SRC-SD results in a suboptimal detection performance. The impact of this suboptimality is quantified in Figure 4. Note that the SER curves of SRC-SD

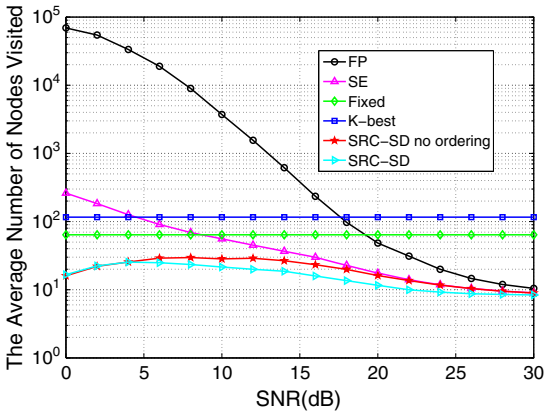

Figure 3. Complexity comparison of different sphere decoders for a 4 × 4 16-QAM MIMO system. QAM, quadrature amplitude modulation; MIMO, multiple-input multiple-output; FP, Fincke–Pohst; SE, Schnorr–Euchner; SRC-SD, SNR-dependent radius control sphere decoder.

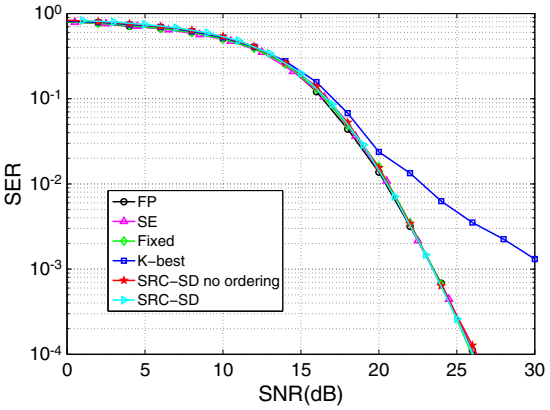

Figure 4. Performance comparison of different sphere decoders for a 4 × 4 16-QAM MIMO system. QAM, quadrature amplitude modulation; MIMO, multiple-input multiple-output; FP, Fincke–Pohst; SE, Schnorr–Euchner; SRC-SD, SNR-dependent radius control sphere decoder.

(with/without ordering), FP and SE are almost identical. The FP, Fixed and SE sphere decoders are full ML detectors. Clearly, SRC-SD achieves a near-ML performance, and also outperforms K-best, especially in the high SNR region. For instance, at an SER of 10^{-3}, SRC-SD gains 7 dB over K-best. Consequently, on the basis of performance and complexity, the new SRC-SD outperforms the Fixed and K-best sphere decoders.

6.2. Detection for coded multiple-input multiple-output system

We next assess the advantages of SRC-SD in a coded MIMO system. The performance measured by the bit error rate and the complexity for a 4×4 coded MIMO system are investigated. The naive LSD is compared with LSRC-SD for several values of the parameter C_0. The systematic recursive convolutional code with rate $R = 1/2$ is exploited to encode the transmitted bits sequence $\mathbf{b}$ with the frame length $M_b = 8192$, where the feed-forward and feedback-generating polynomials are $G_1(D) = 1 + D^2$ and $G_2(D) = 1 + D + D^2$ with memory length 2 [24]. A random interleaver is exploited here. The SNR is used as the Horizontal axis as defined by E_s/N_0.

To choose the best C_0, the performance and complexity comparison of LSRC-SD for different values of C_0 is shown. On the basis of the idea of SRC-SD, by increasing C_0, more nodes are pruned in the searching process, which achieves much lower complexity. The bit error rate performance is also impacted by this parameter. Thus, a proper value for C_0 may be found to attain a nice trade-off between performance and complexity. From Table I, by using four iterations, the performance becomes closer to that of the naive LSD when C_0 decreases. To maintain the performance, a smaller value should be chosen for C_0.

Table I. Performance comparison for different C_0 for a 4 × 4 16-QAM coded MIMO system with $M_b = 8192$ transmitted bits and a maximum of four iterations.

	LSD	LSRC-SD ($C_0 = 1$)	LSRC-SD ($C_0 = 2$)	LSRC-SD ($C_0 = 3$)	LSRC-SD ($C_0 = 5$)	LSRC-SD ($C_0 = 10$)
SNR = 8 dB	0.12010	0.11800	0.1398	0.13170	0.1356	0.16590
SNR = 8.5 dB	0.06390	0.06350	0.0632	0.07080	0.0799	0.10045
SNR = 9 dB	0.01470	0.01460	0.0194	0.02269	0.0284	0.04300
SNR = 9.5 dB	0.00435	0.00450	0.0060	0.00789	0.0093	0.01760
SNR = 10 dB	0.00190	0.00195	0.0029	0.00366	0.0048	0.00810

SNR, signal-to-noise ratio; LSD, list version of sphere decoder; LSRC-SD, list SNR-dependent radius control sphere decoder; QAM, quadrature amplitude modulation; MIMO, multiple-input multiple-output.

Table II. Complexity comparison for different C_0 for a 4×4 16-QAM coded MIMO system with $M_b = 8192$ transmitted bits.

	LSD	LSRC-SD ($C_0 = 1$)	LSRC-SD ($C_0 = 2$)	LSRC-SD ($C_0 = 3$)	LSRC-SD ($C_0 = 5$)	LSRC-SD ($C_0 = 10$)
SNR = 8 dB	4280.2	2561.6	2111.8	1860.5	1571.9	1199.9
SNR = 8.5 dB	4243.4	2624.9	2192.4	1914.4	1633.4	1257.5
SNR = 9 dB	4241.3	2675.8	2240.8	1982.0	1688.6	1314.1
SNR = 9.5 dB	4196.4	2736.7	2302.7	2043.9	1737.8	1381.6
SNR = 10 dB	4190.7	2767.1	2374.7	2121.6	1804.6	1435.7

SNR, signal-to-noise ratio; LSD, list version of sphere decoder; LSRC-SD, list SNR-dependent radius control sphere decoder; QAM, quadrature amplitude modulation; MIMO, multiple-input multiple-output.

The complexity for LSRC-SD with different C_0 is given in Table II. As C_0 increases, the complexity decreases more. For example, the average number of nodes visited are about 1.7×10^3 for $C_0 = 5$, around 2×10^3 with $C_0 = 3$, and approximately 2.2×10^3 with $C_0 = 2$. Therefore, to maintain the performance and reduce the complexity, $C_0 = 2$ should be chosen in this case. Similarly, an appropriate value for other MIMO systems can be found after several trials.

6.3. Detection for multiple-input multiple-output-relay networks

To confirm the benefits of SRC-SD for MIMO-relay networks, its performance and the complexity are evaluated for both DF and AF relays. The number of relays is one or two. The proposed SRC-SD is compared with Fixed, the original SE and CPD [29]. In what follows, it is assumed that $d_{sd} = d_{sr}^{(i)} + d_{rd}^{(i)}$ with $\frac{d_{sr}^{(i)}}{d_{sd}} = 0.2,\ i \in \{1, 2, \ldots N_{re}\}$, the path loss exponent $\alpha = 3$ and $\mu = 0.5$.

Let us first evaluate the SER performance. See Figure 5, which consider the Fixed, SRC-SD and SE sphere decoders. Direct source-to-destination transmissions also occur. The horizontal axis is the transmit power. We set $p = 1$ for Fixed [9] and $C_0 = 10$ for the new SRC-SD. For cooperative partial detection (CPD), we let the expansion factor be 3 [29]. Note that for both the one-relay case and the two-relay case with DF, the SRC-SD, SE and Fixed sphere decoders performs identically. This finding confirms the near-ML performance of SRC-SD. In contrast, CPD incurs performance penalties. For example, for the one-relay case, at an SER of 10^{-3}, it loses 5 dB performance and worse than SRC-SD. Clearly, the SER performance improves when the number of relays increases.

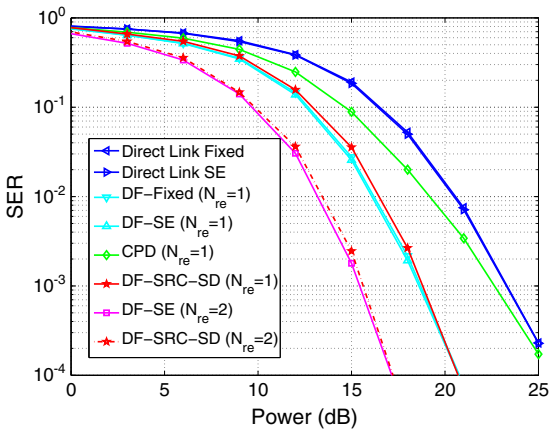

Figure 5. Error probability of sphere detection for a 4 × 4 16-QAM MIMO-relay network. QAM, quadrature amplitude modulation; MIMO, multiple-input multiple-output; SE, Schnorr–Euchner; DF, decode-and-forward; CPD, cooperative partial detection; SRC-SD, signal-to-noise ratio-dependent radius control sphere decoder.

Trans. Emerging Tel. Tech. **26**:389–402 (2015)
DOI: 10.1002/ett

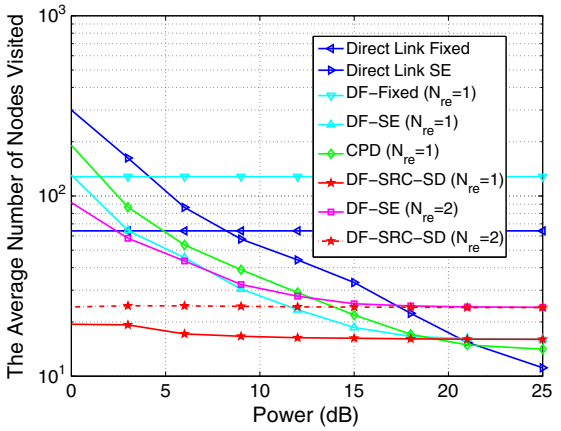

Figure 6. Complexity comparison of sphere detection for a 4 × 4 16-QAM MIMO-relay network. QAM, quadrature amplitude modulation; MIMO, multiple-input multiple-output; SE, Schnorr–Euchner; DF, decode-and-forward; CPD, cooperative partial detection; SRC-SD, signal-to-noise ratio-dependent radius control sphere decoder.

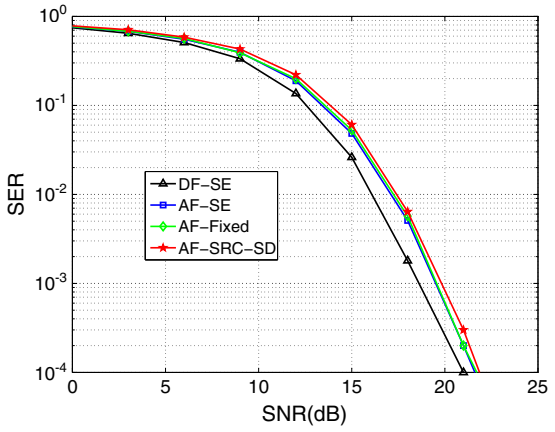

Figure 7. Performance comparison of sphere detection for a 4 × 4 16-QAM MIMO-relay network. QAM, quadrature amplitude modulation; MIMO, multiple-input multiple-output; SE, Schnorr–Euchner; DF, decode-and-forward; AF, amplify-and-forward; SRC-SD, signal-to-noise ratio-dependent radius control sphere decoder.

This result confirms the benefit of using relays to increase the reliability.

The complexity comparison for the same setup shown in Figure 5 is depicted in Figure 6. For the single-relay case, SRC-SD reduces the complexity compared with the CPD, Fixed and SE sphere decoders, and approaches the complexity of SE when the power increases (to higher than 15 dB). For example, at an SNR of 0 dB, SRC-SD visits only 19 nodes, whereas the CPD, Fixed and SE algorithms visit 190, 128 and 130 nodes, respectively. SRC-SD also achieves lower complexity than that of the direct link with SE and Fixed for the lower power region, whereas it has slightly higher complexity than that of the direct transmission when the power is larger than 21 dB. This result is caused by the path loss because of the long distance. For the two-relay network, SRC-SD reduces the complexity compared with that of SE. To check the variability of the complexity here, notice that for both one-relay and two-relay networks, SRC-SD obtains a roughly flat complexity curve as a function of the SNR. For these two cases, it can be shown by using Equation (15) that the variability indexes of SRC-SD are 6.5×10^{-5} and 5.7×10^{-3}, respectively. Our results demonstrate that SRC-SD is an effective detection algorithm for multibranch MIMO-relay networks, with the advantage of roughly fixed, low complexity.

Both the DF and AF cases are considered in Figure 7 and 8. Figure 7 compares the performances of the SRC-SD, SE and Fixed algorithms in one-relay AF and DF systems. In AF relaying, both the SRC-SD and Fixed sphere decoders perform close to that of SE, which is the optimal decoder. In DF relaying, SE achieves a performance gain of 1.5 dB than that in AF.

A complexity comparison for the same setup is also shown in Figure 8. The AF SRC-SD system has lower

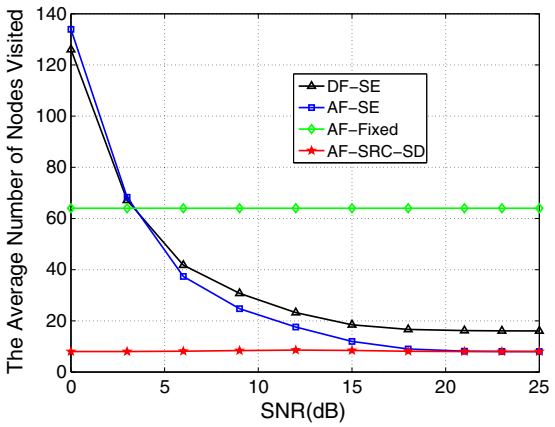

Figure 8. Complexity comparison of sphere detection for a 4 × 4 16-QAM MIMO-relay network. QAM, quadrature amplitude modulation; MIMO, multiple-input multiple-output; SE, Schnorr–Euchner; DF, decode-and-forward; AF, amplify-and-forward; SRC-SD, signal-to-noise ratio-dependent radius control sphere decoder.

complexity than the SE and Fixed sphere decoders, just as in DF relaying (Figure 6). Especially, in the low-power region, SRC-SD significantly reduces complexity. For example, at 0 dB, it is only 6% of that of SE. Thus, systems that operate in the low SNR region may particularly benefit from the use of SRC-SD. As expected, however, both the SRC-SD and SE algorithms have the same level of complexity in the high SNR region ($>$ 20 dB). It is interesting to compare the DF SE and AF SRC-SD systems. The complexity saving varies from 93.6% to 52%. The variability index η is found to be 1.9×10^{-4} for SRC-SD, which demonstrates roughly fixed complexity.

These results again confirm that SRC-SD reduces the complexity and its variability.

7. CONCLUSIONS

This paper proposed an SRC-SD with reduced complexity, reduced variability of complexity, and near-ML performance. The search radius is tightened by a heuristic SNR-dependent factor. The resulting algorithm outperforms existing detectors such as the K-best and Fixed sphere decoders in terms of SER but also saves complexity. For coded MIMO systems, we proposed, as a soft extension of the new SRC-SD, LSRC-SD for generating the candidate list. This LSRC-SD algorithm further improves the complexity of detection and decoding at a negligible performance loss. Signal detection for AF and DF MIMO-relay networks was also investigated by deriving the ML detection rules. The simulation results confirmed the benefits of the proposed SRC-SD with a near-ML performance and roughly constant complexity.

APPENDIX A

According to the norm expansion $||\mathbf{H}||^2 = \mathbf{H}^H\mathbf{H}$, the Equation (21) is expanded as

$$\begin{aligned}\hat{\mathbf{s}}_d &= \arg\min_{\mathbf{s}_s\in\mathcal{Q}^{N_s}}\left(\sum_{i=1}^{N_{re}}||\mathbf{y}_{rd}^{(i)}-\mathbf{H}_{rd}^{(i)}\mathbf{s}_s||^2 \right.\\ &\qquad \left.+||\mathbf{y}_d-\mathbf{H}_{sd}\mathbf{s}_s||^2\right).\\ &= \arg\min_{\mathbf{s}_s\in\mathcal{Q}^{N_s}}\left[\sum_{i=1}^{N_{re}}\mathbf{y}_{rd}^{(i)H}\mathbf{y}_{rd}^{(i)}+\mathbf{y}_d^H\mathbf{y}_d\right.\\ &\qquad -\mathbf{s}_s^H\left(\sum_{i=1}^{N_{re}}\mathbf{H}_{rd}^{(i)H}\mathbf{y}_{rd}^{(i)}+\mathbf{H}_{sd}^H\mathbf{y}_d\right)\\ &\qquad -\left(\sum_{i=1}^{N_{re}}\mathbf{y}_{rd}^{(i)H}\mathbf{H}_{rd}^{(i)}+\mathbf{y}_d^H\mathbf{H}_{sd}\right)\mathbf{s}_s^H\\ &\qquad \left.+\mathbf{s}_s^H\left(\sum_{i=1}^{N_{re}}\mathbf{H}_{rd}^{(i)H}\mathbf{H}_{rd}^{(i)}+\mathbf{H}_{sd}^H\mathbf{H}_{sd}\right)\mathbf{s}_s\right]\end{aligned} \tag{A1}$$

Assuming $\mathbf{y}'$ and $\mathbf{H}'$ are derived, the ML expression maybe expanded similarly as

$$\begin{aligned}\hat{\mathbf{s}}_d &= \arg\min_{\mathbf{s}_s\in\mathcal{Q}^{N_s}}||\mathbf{y}'-\mathbf{H}'\mathbf{s}_s||^2\\ &= \arg\min_{\mathbf{s}_s\in\mathcal{Q}^{N_s}}\left(\mathbf{y}'^H\mathbf{y}'-\mathbf{s}_s^H\mathbf{H}'^H\mathbf{y}'\right.\\ &\qquad \left.-\mathbf{y}'^H\mathbf{H}'\mathbf{s}_s+\mathbf{s}_s^H\mathbf{H}'^H\mathbf{H}'\mathbf{s}_s\right)\end{aligned} \tag{A2}$$

By comparing Equations (A1) and (A2), it is clear that

$$\mathbf{H}'^H\mathbf{H}' = \sum_{i=1}^{N_{re}}\mathbf{H}_{rd}^{(i)H}\mathbf{H}_{rd}^{(i)}+\mathbf{H}_{sd}^H\mathbf{H}_{sd} \tag{A3a}$$

$$\mathbf{H}'^H\mathbf{y}' = \sum_{i=1}^{N_{re}}\mathbf{H}_{rd}^{(i)H}\mathbf{y}_{rd}^{(i)}+\mathbf{H}_{sd}^H\mathbf{y}_d \tag{A3b}$$

Further, because of $\left(\sum_{i=1}^{N_{re}}\mathbf{H}_{rd}^{(i)H}\mathbf{H}_{rd}^{(i)}+\mathbf{H}_{sd}^H\mathbf{H}_{sd}\right)^H = \sum_{i=1}^{N_{re}}\mathbf{H}_{rd}^{(i)H}\mathbf{H}_{rd}^{(i)}+\mathbf{H}_{sd}^H\mathbf{H}_{sd}$, Equation (A3a) could be shown as

$$\begin{aligned}\mathbf{H}'^H\mathbf{H}' &= \left[\left(\sum_{i=1}^{N_{re}}\mathbf{H}_{rd}^{(i)H}\mathbf{H}_{rd}^{(i)}+\mathbf{H}_{sd}^H\mathbf{H}_{sd}\right)^H\right.\\ &\qquad \left.\times\left(\sum_{i=1}^{N_{re}}\mathbf{H}_{rd}^{(i)H}\mathbf{H}_{rd}^{(i)}+\mathbf{H}_{sd}^H\mathbf{H}_{sd}\right)\right]^{\frac{1}{2}},\\ &= \left[\left(\sum_{i=1}^{N_{re}}\mathbf{H}_{rd}^{(i)H}\mathbf{H}_{rd}^{(i)}+\mathbf{H}_{sd}^H\mathbf{H}_{sd}\right)^{\frac{1}{2}}\right]^H\\ &\qquad \times\left(\sum_{i=1}^{N_{re}}\mathbf{H}_{rd}^{(i)H}\mathbf{H}_{rd}^{(i)}+\mathbf{H}_{sd}^H\mathbf{H}_{sd}\right)^{\frac{1}{2}}\end{aligned} \tag{A4}$$

thus, the equivalent channel matrix $\mathbf{H}'$ is

$$\mathbf{H}' = \left(\sum_{i=1}^{N_{re}}\mathbf{H}_{rd}^{(i)H}\mathbf{H}_{rd}^{(i)}+\mathbf{H}_{sd}^H\mathbf{H}_{sd}\right)^{1/2} \tag{A5}$$

where $\mathbf{H}' = \mathbf{H}'^H$.

According to the equivalent channel matrix, Equations (A1) and (A2), the equivalent received signal $\mathbf{y}'$ are derived as

$$\begin{aligned}\mathbf{y}' &= (\mathbf{H}'^H)^{-1}\left(\sum_{i=1}^{N_{re}}\mathbf{H}_{rd}^{(i)H}\mathbf{y}_{rd}^{(i)}+\mathbf{H}_{sd}^H\mathbf{y}_{sd}\right),\\ &= (\mathbf{H}')^{-1}\left(\sum_{i=1}^{N_{re}}\mathbf{H}_{rd}^{(i)H}\mathbf{y}_{rd}^{(i)}+\mathbf{H}_{sd}^H\mathbf{y}_{sd}\right)\end{aligned} \tag{A6}$$

REFERENCES

1. Murugan A, El Gamal H, Damen M, Caire G. A unified framework for tree search decoding: rediscovering the sequential decoder. *IEEE Transactions on Information Theory* 2006; **52**(3): 933–953. DOI: 10.1109/TIT.2005.864418.

2. Cui T, Tellambura C. Generalized feedback detection for spatial multiplexing multi-antenna systems. *IEEE Transactions on Wireless Communications* 2008; **7**(2): 594–603. DOI: 10.1109/TWC.2008.060513.
3. Kim J-S, Moon S-H, Lee I. A new reduced complexity ML detection scheme for MIMO systems. *IEEE Transactions on Communications* 2010; **58**(4): 1302–1310. DOI: 10.1109/TCOMM.2010.04.080450.
4. Cui T, Ho T, Tellambura C. Statistical pruning for near maximum likelihood detection of MIMO systems. In *Proceedings of IEEE International Conference on Communications (ICC)*, Glasgow, Scotland, 2007; 5462–5467, DOI: 10.1109/ICC.2007.905.
5. Cui T, Tellambura C. Approximate ML detection for MIMO systems using multistage sphere decoding. *IEEE Signal Processing Letters* 2005; **12**(3): 222–225. DOI: 10.1109/LSP.2004.842263.
6. Shim B, Kang I. Sphere decoding with a probabilistic tree pruning. *IEEE Transactions on Signal Processing* 2008; **56**(10): 4867–4878. DOI: 10.1109/TSP.2008.923808.
7. Shim B, Kang I. On further reduction of complexity in tree pruning based sphere search. *IEEE Transactions on Communications* 2010; **58**(2): 417–422. DOI: 10.1109/TCOMM.2010.02.080340.
8. Guo Z, Nilsson P. Algorithm and implementation of the K-best sphere decoding for MIMO detection. *IEEE Journal on Selected Areas in Communications* 2006; **24**(3): 491–503. DOI: 10.1109/JSAC.2005.862402.
9. Barbero L, Thompson J. Fixing the complexity of the sphere decoder for MIMO detection. *IEEE Transactions on Wireless Communications* 2008; **7**(6): 2131–2142. DOI: 10.1109/TWC.2008.060378.
10. Su K, Wassell I. A new ordering for efficient sphere decoding. *Proceedings of International Conference on Communications (ICC)* 2005; **3**: 1906–1910. DOI: 10.1109/ICC.2005.1494671.
11. Cui T, Tellambura C. Joint data detection and channel estimation for OFDM systems. *IEEE Transactions on Communications* 2006; **54**(4): 670–679. DOI: 10.1109/TCOMM.2006.873075.
12. Cui T, Tellambura C. An efficient generalized sphere decoder for rank-deficient MIMO systems. *IEEE Communications Letters* 2005; **9**(5): 423–425. DOI: 10.1109/LCOMM.2005.1431159.
13. Wiesel A, Mestre X, Pages A, Fonollosa J. Efficient implementation of sphere demodulation. In *Proceedings of IEEE Workshop on Signal Processing Advances in Wireless Communications*, Rome, Italy, 2003; 36–40, DOI: 10.1109/SPAWC.2003.1318917.
14. Han S, Cui T, Tellambura C. Improved K-Best sphere detection for uncoded and coded MIMO systems. *IEEE Wireless Communications Letters* 2012; **1**(5): 472–475. DOI: 10.1109/WCL.2012.070312.120472.
15. Anderson J, Mohan S. Sequential coding algorithms: a survey and cost analysis. *IEEE Transactions on Communications* 1984; **32**(2): 169–176. DOI: 10.1109/TCOM.1984.1096023.
16. Zhang W. *State-Space Search: Algorithms, Complexity, Extensions, and Applications*. Springer-Verlag New York, Inc.: New York, 1999.
17. Barbero L, Thompson J. A fixed-complexity MIMO detector based on the complex sphere decoder. In *Proceedings of IEEE 7th Workshop on Signal Processing Advances in Wireless Communications*, Cannes, France, 2006; 1–5, DOI: 10.1109/SPAWC.2006.346388.
18. Gowaikar R, Hassibi B. Efficient statistical pruning for maximum likelihood decoding. *Proceedings of IEEE International Conference on Acoustics Speech and Signal Processing (ICASSP)* 2003; **5**: 49–52. DOI: 10.1109/ICASSP.2003.1199865.
19. Zhao W, Giannakis G. Sphere decoding algorithms with improved radius search. *IEEE Transactions on Communications* 2005; **53**(7): 1104–1109. DOI: 10.1109/TCOMM.2005.851590.
20. Guo Z, Nilsson P. Reduced complexity Schnorr–Euchner decoding algorithms for MIMO systems. *IEEE Communications Letters* 2004; **8**(5): 286–288. DOI: 10.1109/LCOMM.2004.827376.
21. Younis A, Mesleh R, Haas H, Grant P. Reduced complexity sphere decoder for spatial modulation detection receivers. In *Proceedings of the IEEE Global Communications Conference (GLOBECOM)*, Miami, USA, 2010; 1–5, DOI: 10.1109/GLOCOM.2010.5683993.
22. Lai I-W, Ascheid G, Meyr H, Chiueh T-D. Efficient channel-adaptive MIMO detection using just-acceptable error rate. *IEEE Transactions on Wireless Communications* 2011; **10**(1): 73–83. DOI: 10.1109/TWC.2010.101810.091129.
23. Wu YH, Liu YT, Chang H-C, Liao Y-C, Chang H-C. Early-pruned K-best sphere decoding algorithm based on radius constraints. In *Proceedings of International Conference on Communications (ICC)*, Beijing, China, 2008; 4496–4500, DOI: 10.1109/ICC.2008.843.
24. Hochwald B, ten Brink S. Achieving near-capacity on a multiple-antenna channel. *IEEE Transactions on Communications* 2003; **51**(3): 389–399. DOI: 10.1109/TCOMM.2003.809789.
25. Barbero L, Thompson J. Extending a fixed-complexity sphere decoder to obtain likelihood information for turbo-MIMO systems. *IEEE Transactions on Vehicular Technology* 2008; **57**(5): 2804–2814. DOI: 10.1109/TVT.2007.914064.
26. Nosratinia A, Hunter T, Hedayat A. Cooperative communication in wireless networks. *IEEE*

Communications Magazine 2004; **42**(10): 74–80. DOI: 10.1109/MCOM.2004.1341264.

27. Fan Y, Thompson J. MIMO configurations for relay channels: theory and practice. *IEEE Transactions on Wireless Communications* 2007; **6**(5): 1774–1786. DOI: 10.1109/TWC.2007.360379.
28. Chen J, Yu X, Kuo C-C. V-BLAST receiver and performance in MIMO relay networks with imperfect CSI. In *Proceedings of International Conference on Communications (ICC)*, Beijing, China, 2008; 4436–4440, DOI: 10.1109/ICC.2008.832.
29. Amiri K, Wu M, Cavallaro J, Lilleberg J. Cooperative partial detection using MIMO relays. *IEEE Transactions on Signal Processing* 2011; **59**(10): 5039–5049. DOI: 10.1109/TSP.2011.2157498.
30. Tuchler M, Singer AC. Turbo equalization: an overview. *IEEE Transactions on Information Theory* 2011; **57**(2): 920–952. DOI: 10.1109/TIT.2010.2096033.
31. Laneman J, Tse D, Wornell G. Cooperative diversity in wireless networks: efficient protocols and outage behavior. *IEEE Transactions on Information Theory* 2004; **50**(12): 3062–3080. DOI: 10.1109/TIT.2004.838089.
32. Fincke U, Pohst M. Improved methods for calculating vectors of short length in a lattice, including a complexity analysis. *Mathematics of Computation* 1985; **44**: 463–471.
33. Schnorr CP, Euchner M. Lattice basis reduction: improved practical algorithms and solving subset sum problems. *Mathematics of Computation* 1985; **66**: 181–199.
34. Hassibi B, Vikalo H. On the sphere-decoding algorithm I. expected complexity. *IEEE Transactions on Signal Processing* 2005; **53**(8): 2806–2818. DOI: 10.1109/TSP.2005.850352.
35. Wolniansky P, Foschini G, Golden G, Valenzuela R. V-BLAST: an architecture for realizing very high data rates over the rich-scattering wireless channel. In *Proceedings of URSI International Symposium on Signals, Systems and Electonics (ISSSE)*, Pisa, Italy, 1998; 295–300, DOI: 10.1109/ISSSE.1998.738086.
36. Ma Z, Honary B, Fan P, Larsson E. Stopping criterion for complexity reduction of sphere decoding. *IEEE Communications Letters* 2009; **13**(6): 402–404. DOI: 10.1109/LCOMM.2009.090112.
37. Robertson P, Villebrun E, Hoeher P. A comparison of optimal and sub-optimal MAP decoding algorithms operating in the log domain. *Proceedings of International Conference on Communications (ICC)* 1995; **2**: 1009–1013. DOI: 10.1109/ICC.1995.524253.